Otto Focus
Research Scientist
Corporation ABC
123 Industry Road
Austenite, MN 12345

Report Date: April 1, 2015
Date Submitted: April 1, 2015
MEE Project: ZZ0001
Sample ID: 12345
P.O. No.: 54321

PROJECT TITLE: Evaluation of a Failed Right Lateral Water Wall Tube

INTRODUCTION

A metallurgical evaluation was requested to investigate a crack in a right lateral water wall tube. The primary objective of the evaluation was to determine the failure mechanism of the tube. Secondary objectives were to characterize the tube material for degradation in service and identify any material anomalies that may have contributed to the failure. No material specifications nor operating conditions for the tube were provided.

SUMMARY AND CONCLUSIONS

There was an approximately 1-in. long longitudinal crack through the tube wall near the center of the submitted 11-in. long tube section. The crack was assumed to be on the hot side of the tube, which was covered in light brown scale. The cold side of the tube was reddish brown in color and had numerous shallow pits on the outer surface.

The inside surface was entirely covered in adherent reddish-brown deposits. Under the deposits, there were deep pits filled with deposits on the hot side of the tube. Near the crack, the deposits were thicker and had a flaky texture. The composition of the deposit material was consistent with iron oxide.

The through-wall crack in the tube was tight with no significant plastic deformation. At the outer surface, the crack followed a jagged, generally longitudinal path. On the inner surface on the hot side of the tube, there were numerous cracks.

A metallographically-prepared cross section of the tube revealed numerous tight cracks in the tube wall near the inside surface on the hot side of the tube. The cracking was discontinuous and followed the material grain boundaries. The cracks were more concentrated and penetrated further into the wall thickness near a large pit. Intergranular cracks within the wall were consistent with a fracture mechanism of hydrogen damage.

The microstructure of the tube metal was a ferrite matrix with narrow bands of small pearlite islands. This microstructure is consistent with a carbon steel tube in the normalized condition. Other than the cracking, no indications of tube material degradation in service were observed.

The intergranular cracking pattern under thick deposits and the numerous cracks within the wall thickness indicated that the tube failed due to hydrogen damage. Failures due to hydrogen damage are commonly caused by either a high or low pH excursion on the water side of the tube. Chemical reactions between a metal and acid or caustic conditions can liberate atomic hydrogen, which diffuses into the steel. In the steel, the hydrogen reacts to form small cracks on the grain boundaries, which eventually coalesce to form a leak through the tube wall.

Most commonly, variations in pH are caused by contamination due to either condenser in-leakage or water contaminants. Preventing contamination, condenser in-leakage, and excessive water-side deposition and scale formation are the most effective ways of preventing hydrogen damage. Periodic tube sampling to is recommended to monitor these conditions.

In summary, the failure mechanism for the tube was hydrogen damage. The hydrogen damage embrittled the tube metal, and initiation and coalescence of intergranular cracks resulted in the tube failure. Preventing contamination, condenser in-leakage, and excessive water-side deposition and scale formation are the most effective ways of preventing hydrogen damage. Other than the hydrogen damage, no material or manufacturing anomalies were observed that would have contributed to the failure.

TEST PROCEDURES

The submitted sample was examined visually at magnifications from 1X to 30X with the aid of a light microscope. Photographs documenting significant observations were taken during the visual examination.

One ring of the tube was cut from an area adjacent to the crack and a second ring was cut from an area away from the crack. Wall thickness measurements were made on the hot side and the cold side of both rings using a point micrometer.

A third ring was cut near the crack, then flattened in a vice. The fracture surface formed when the ring was flattened was examined by scanning electron microscopy (SEM). In conjunction with the SEM examination, qualitative chemical analyses were performed in selected areas of the sample by energy dispersive x-ray spectroscopy (EDS).

A transverse section of the tube near the leak site was mounted in thermosetting epoxy and metallographically prepared. The prepared section was examined as polished and after etching in 2% nital. The examination was performed using light microscopy, and micrographs of representative microstructures were taken.

RESULTS

VISUAL EXAMINATION

A 11-in. long section of a right lateral water wall tube was submitted. The outer surface of one side of the tube had a slightly rough texture and a thin light brown scale, Figure 1. This was assumed to be the hot side of the tube. There was an approximately 1-in. long longitudinal crack near the center of the section on the hot side of the tube, Figure 2.

The cold side of the tube was a dark red-brown color and had numerous small pits on the outer surface, Figure 3.

The inner surface of the tube was entirely covered with adherent dark-red deposits. On the cold side of the tube, the deposits were relatively thin and smooth, Figure 4. On the hot side, the deposits were considerably thicker and had a flaky texture, Figure 5. The outline of the crack on the inside surface was not easily distinguishable under the thick deposits and scale.

WALL THICKNESS MEASUREMENTS

The wall thickness measurements are reported in the following table. The two rings are shown in Figure 6.

Location	Wall Thickness, in. Measured	Average
Near crack - hot side	0.163, 0.187, 0.182	0.177
Near crack - cold side	0.223, 0.222, 0.226	0.224
Away from crack - hot side	0.193, 0.190, 0.207	0.197
Away from crack - cold side	0.221, 0.220, 0.218	0.22

METALLOGRAPHIC EXAMINATION

Transverse sections of both the hot and cold side from a ring containing the crack tip were metallographically prepared, Figure 6a. The results of the examination of these specimens are presented in the following subsections.

Cold side - The outer surface was relatively smooth with a few shallow pits and a thin nonmetallic scale, Figure 7a. The inner surface had a few localized regions of deeper pits, Figure 7b. Some of the pits were filled with nonmetallic deposits and scale.

Hot side - The outer surface had a few shallow pits and a moderately-thick nonmetallic scale,

Figure 8a. The inner surface had a larger, much deeper pit filled with nonmetallic deposits and scale.

There were numerous small, tight cracks in the tube wall near the inner surface of the tube, Figure 8. The highest concentration and deepest penetration of the cracks was located at the large pit. The cracks were discontinuous and followed the contours of the grain boundaries. In some areas, the small cracks had coalesced to form larger cracks, Figures 8 and 9.

The microstructure of the tube metal consisted of a ferrite matrix with narrow bands of small pearlite islands, Figures 10 and 11. This structure was consistent with a carbon steel tube in the normalized condition.

SEM/EDS EXAMINATION

The flattening of the ring section removed produced a fracture through the tube wall on the hot side Figure 12. The microscopic fracture features near the inside surface of the tube consisted of predominantly intergranular fracture with small patches of a dimpled morphology, Figure 13a. These features indicated ductile fracture of the remaining ligaments between the numerous intergranular cracks in the tube wall. The microscopic fracture features near the outer surface were almost entirely dimples indicating a ductile fracture mechanism, Figure 13b.

EDS analysis of the fracture surface detected primarily iron, with smaller concentrations of carbon, manganese and silicon, Figure 14. This composition was consistent with a carbon steel tube material.

Analysis of nonmetallic material scraped from the inner surface on the hot side near the crack detected primarily iron and oxygen, with lesser concentrations of aluminum, carbon, chromium, copper, nickel, phosphorous and zinc, Figures 15 and 16. Thus, the nonmetallic material was predominantly iron oxide. The remaining elements were likely corrosion products for other areas of the boiler, residue of water treatment chemicals, and water contaminants.

SAMPLE DISPOSITION AND DATA STORAGE

The samples from this project will be stored for at least 3 months from the date of this report. Samples may then be discarded unless instructions for return or other disposition are received. All data will be kept on file, and additional report copies can be obtained upon request.

Submitted by:
Mike Rowscope
Senior Materials Engineer

Reviewed by:
E. Val Yuation
Principal Engineer

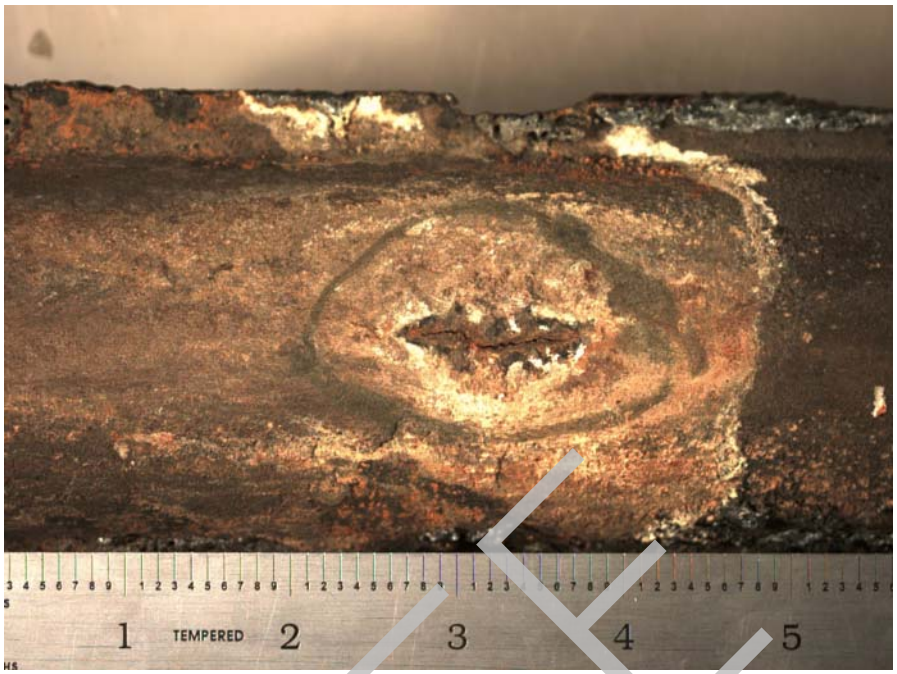

(a)

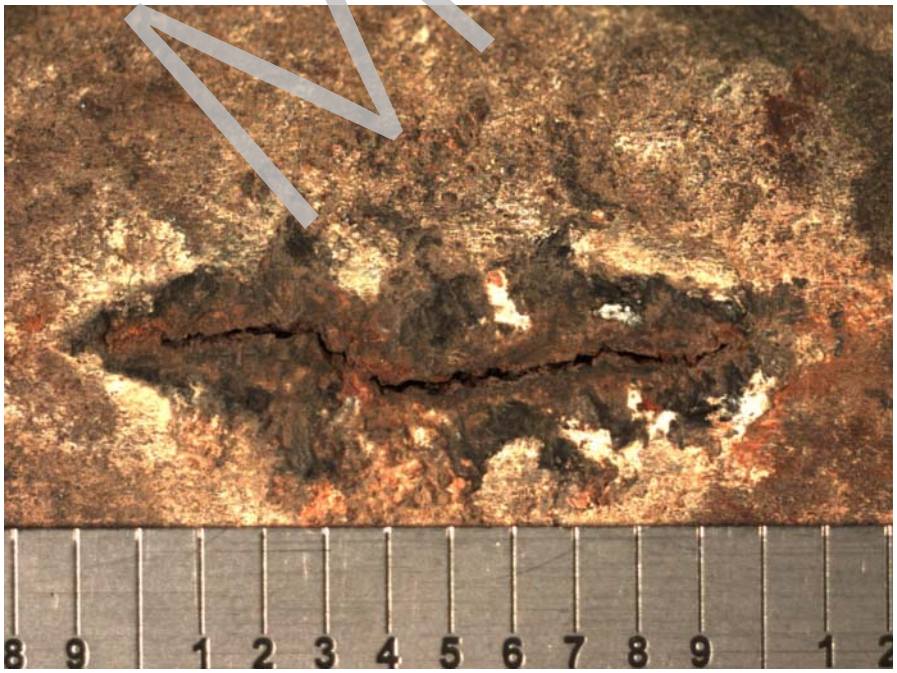

(b)

Figure 2 Crack on the outer surface of the hot side of the tube.

(a)

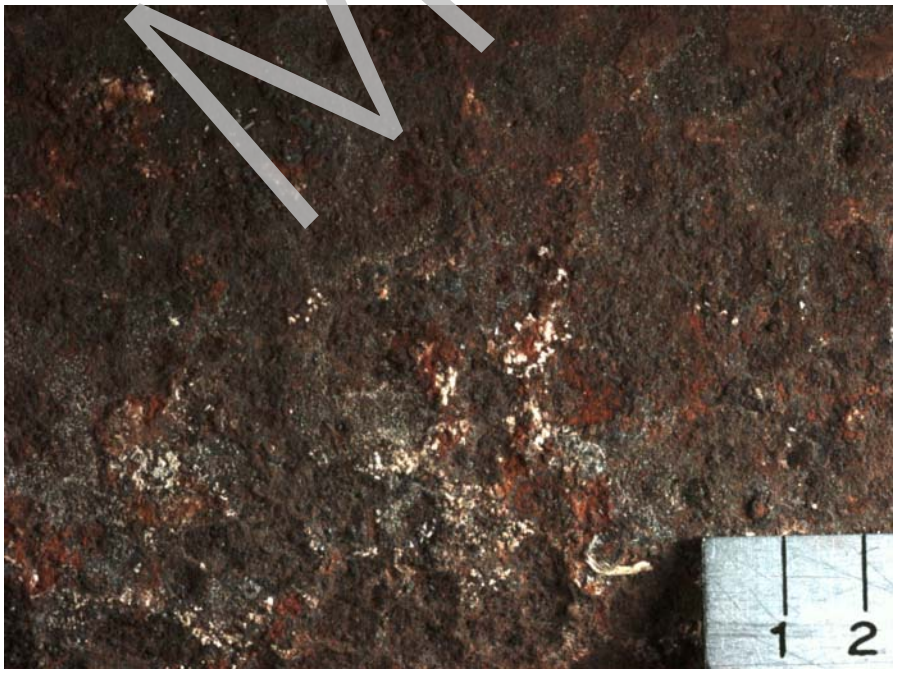

(b)

Figure 3 Cold side of the as-received tube.

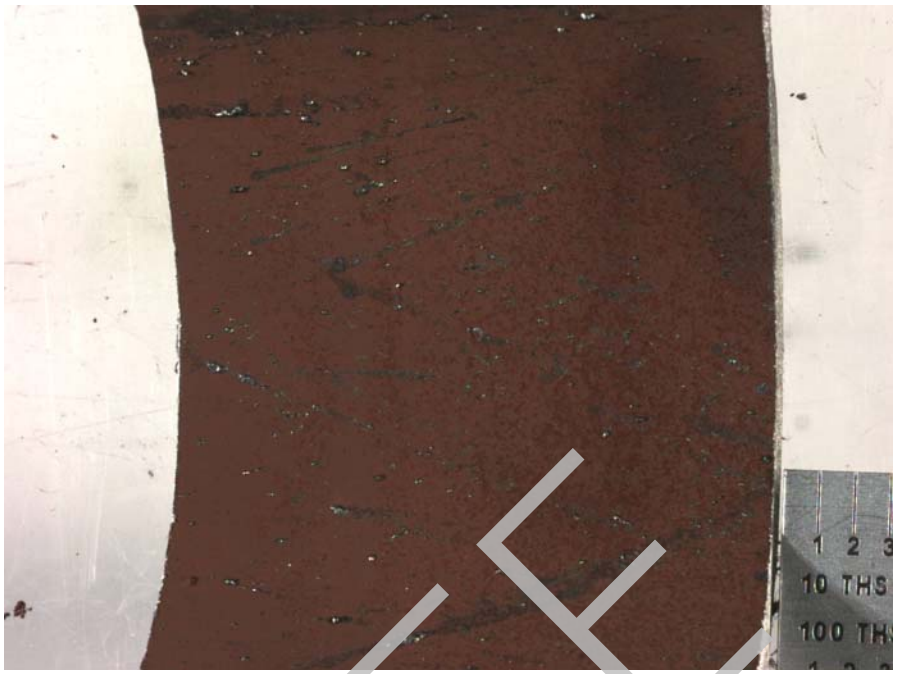

(a)

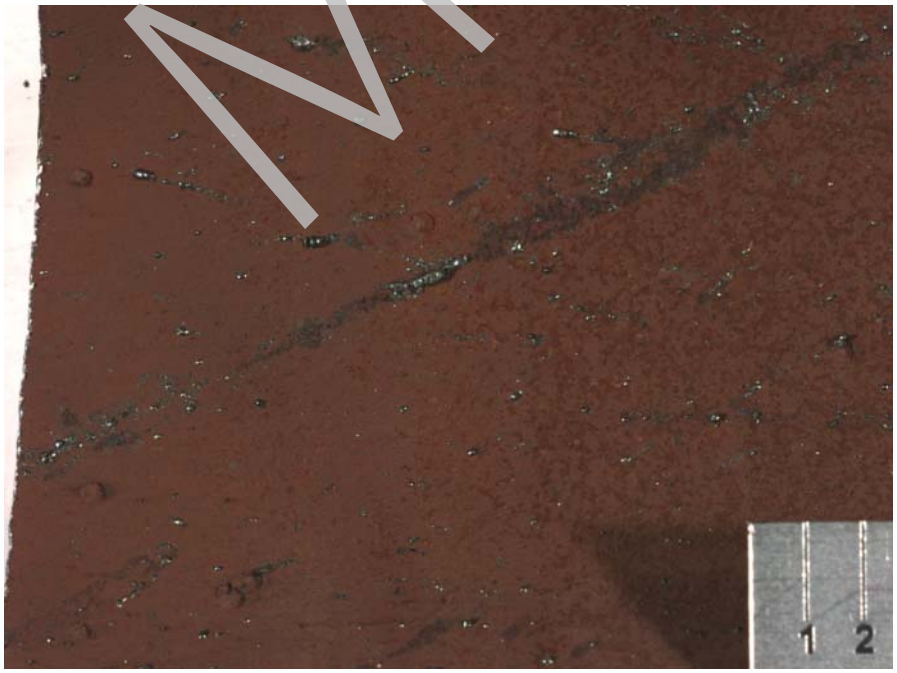

(b)

Figure 4 Deposits on the inner surface of the cold side of the tube.

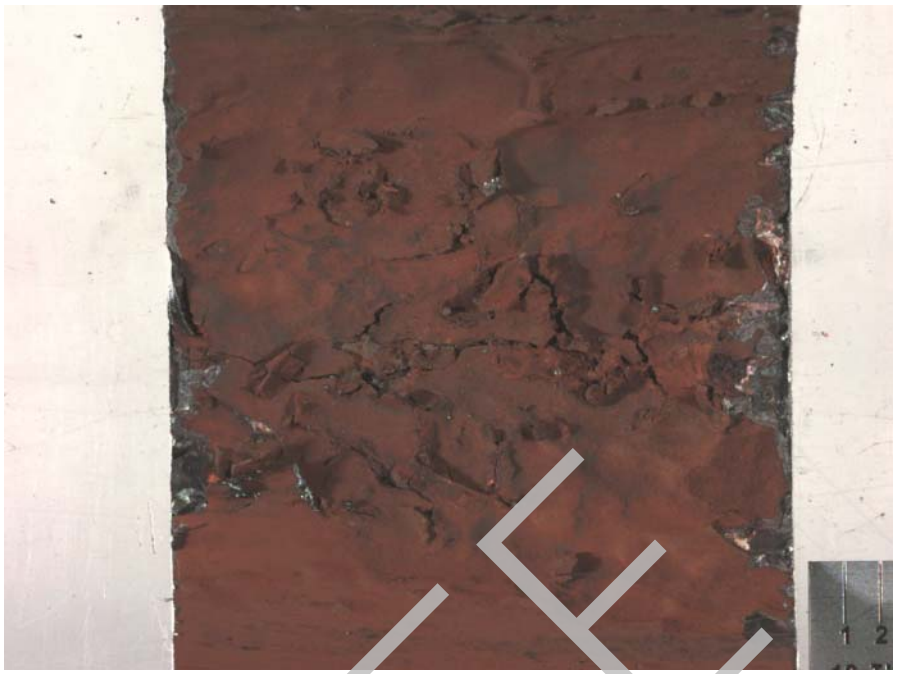

(a)

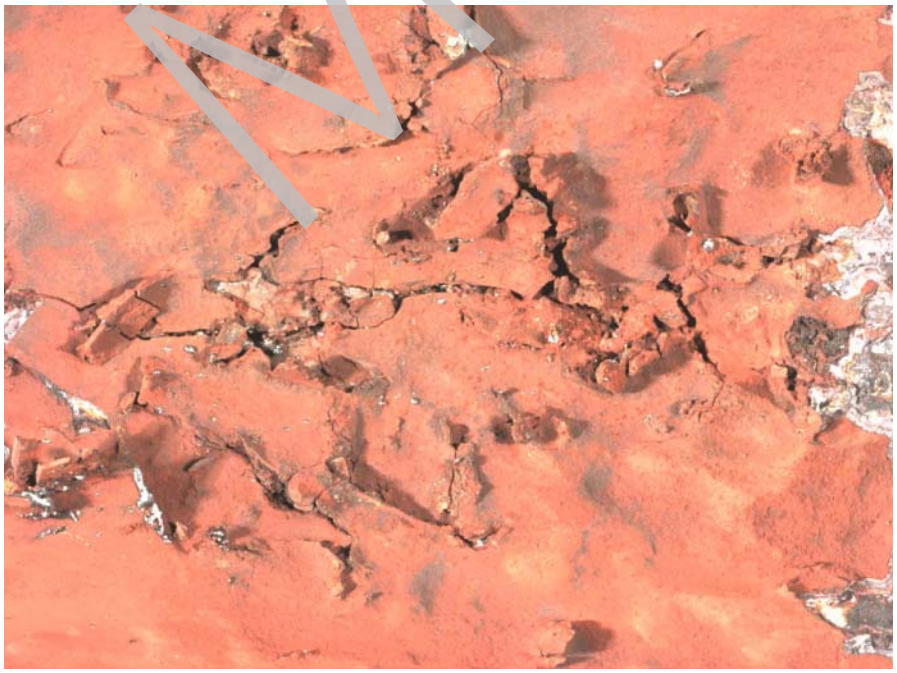

(b)

Figure 5 Deposits and cracking on the inner surface of the hot side of the tube.

(a) Near crack

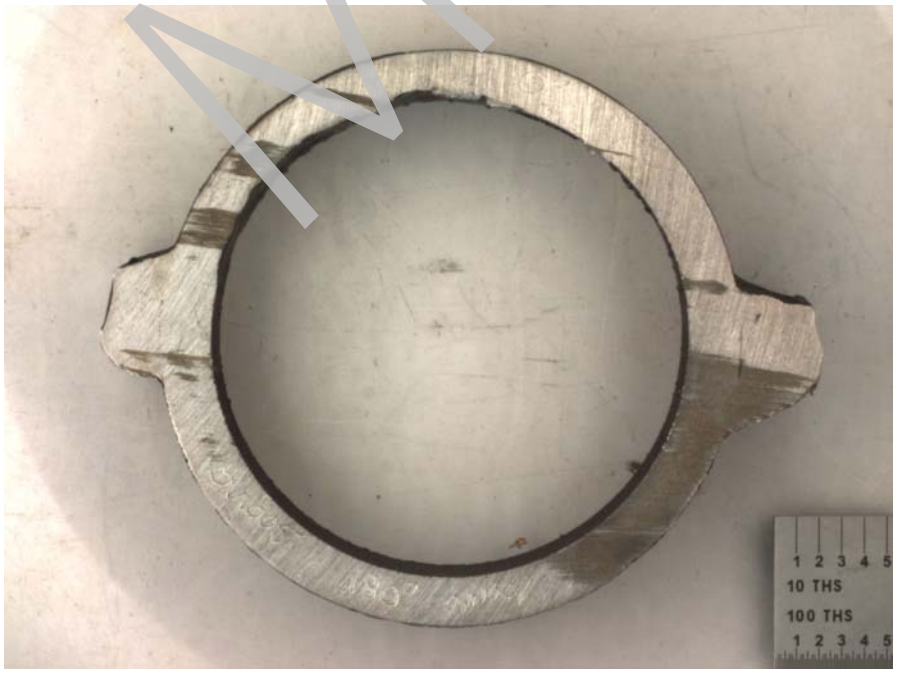

(b) Away from crack

Figure 6 Rings removed from the indicated location for wall thickness measurements. The hot side is at the top of the ring in both images.

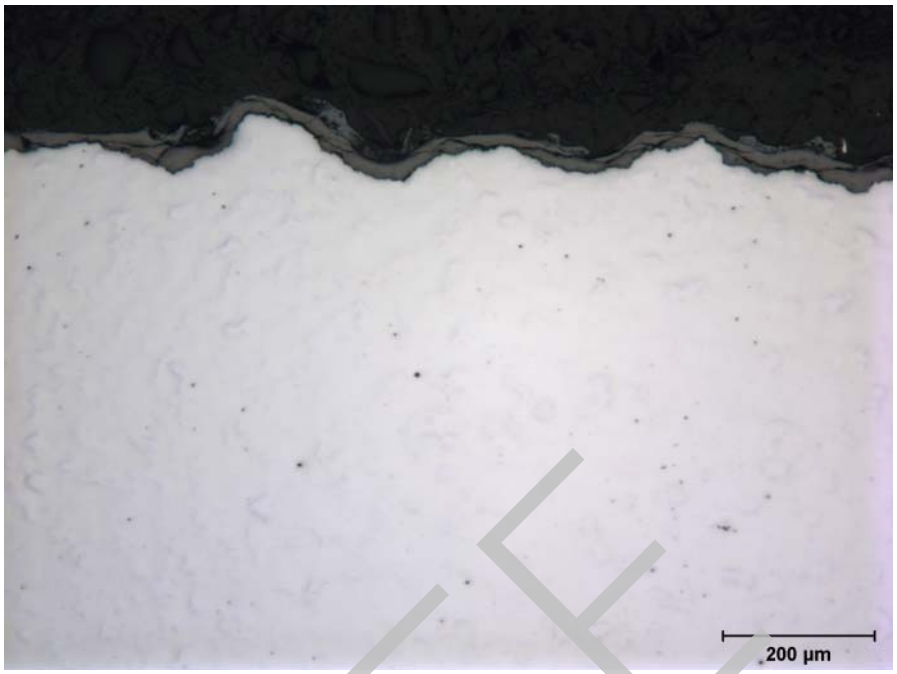

As Polished Magnification: 100X

(a) Outer surface

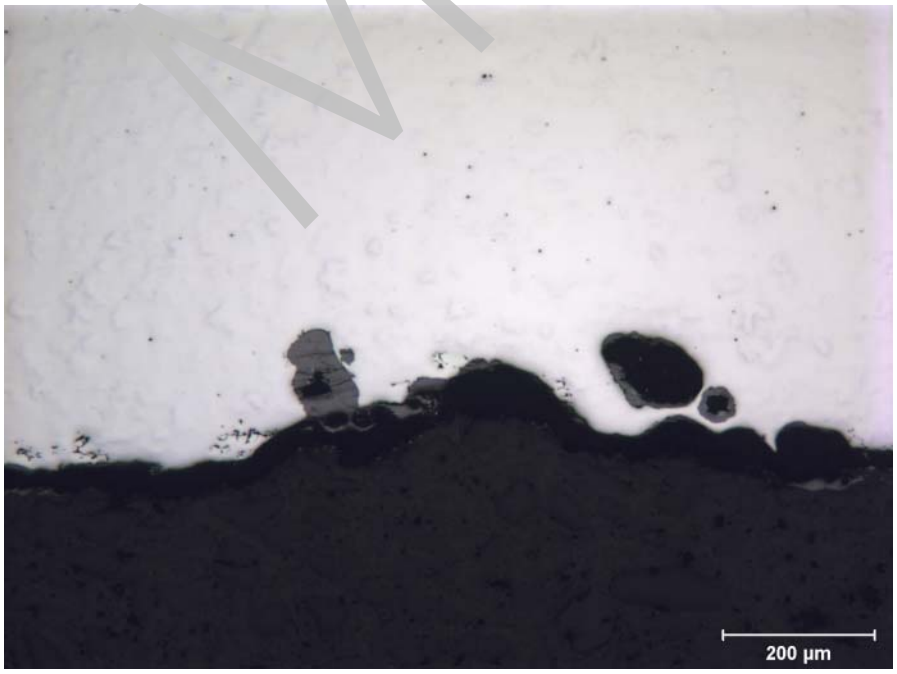

As Polished Magnification: 100X

(b) Inner surface

Figure 7 Cross section at the indicated surfaces on the cold side of the tube.

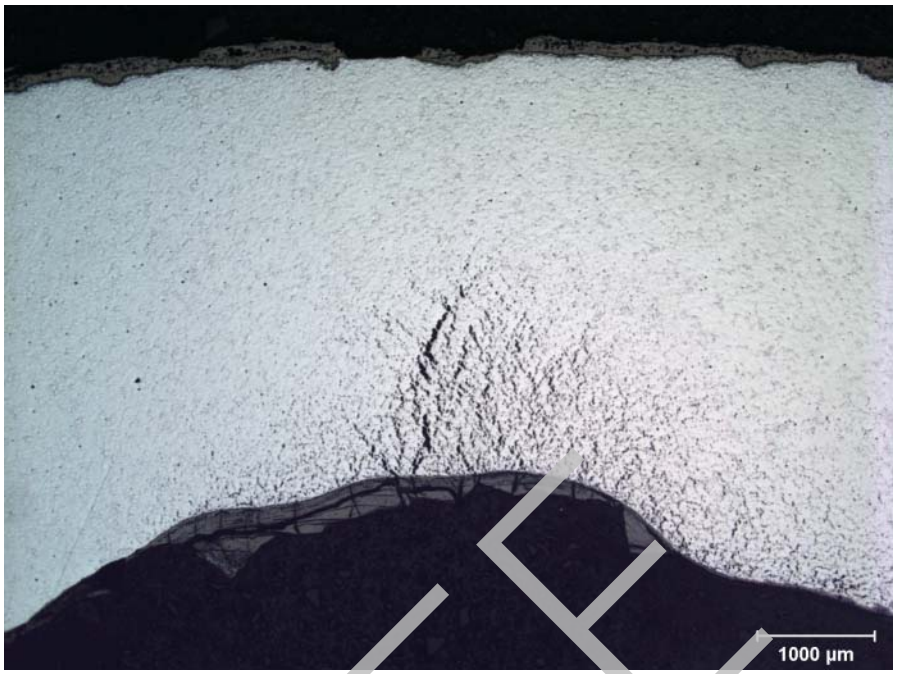

As Polished Magnification: 16X

(a)

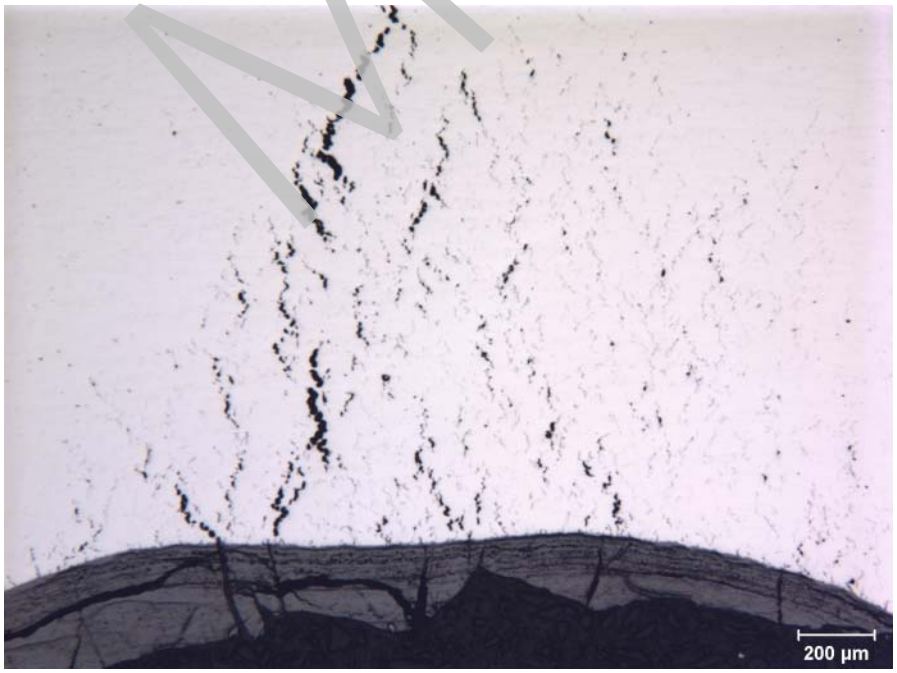

As Polished Magnification: 50X

(b)

Figure 8 Cross section showing cracks in the hot side of the tube.

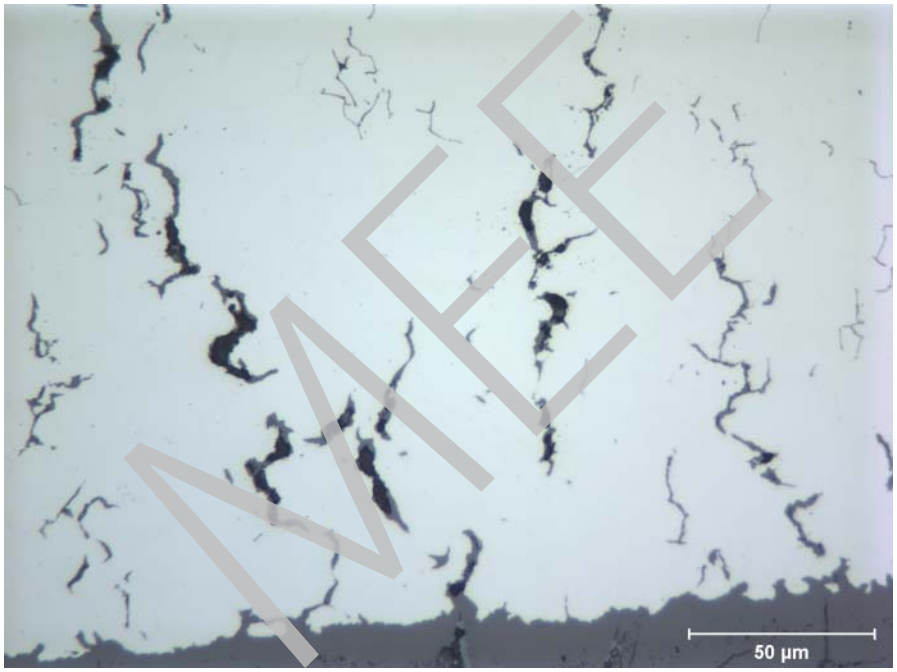

As Polished Magnification: 500X

Figure 9 Cracks near the inside surface on the hot side of the tube.

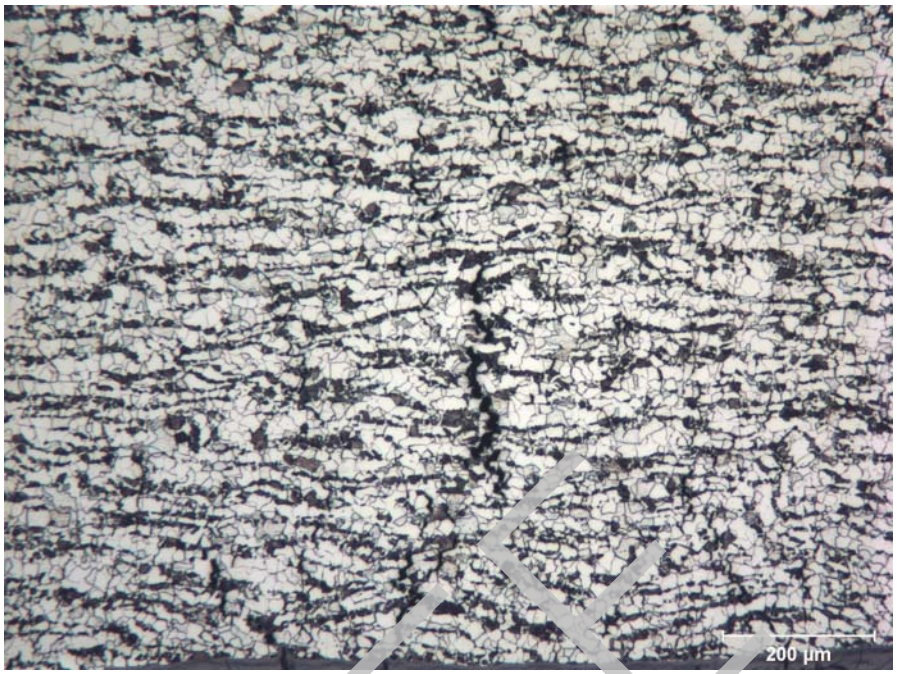

Etchant: 2% Nital Magnification: 100X

(a)

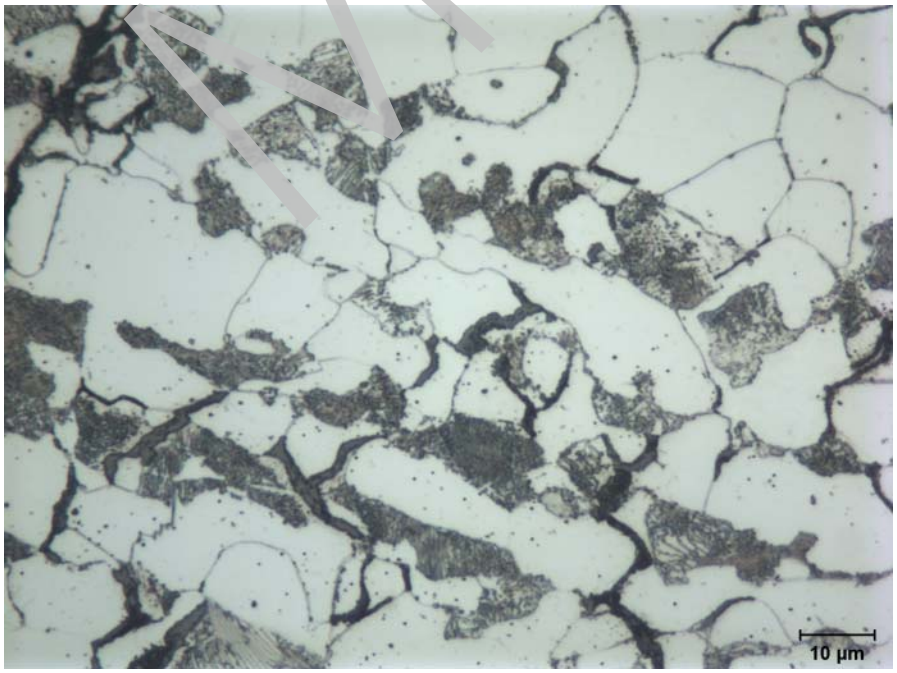

Etchant: 2% Nital Magnification: 1,000X

(b)

Figure 10 Microstructure of the tube metal on the hot side of the tube.

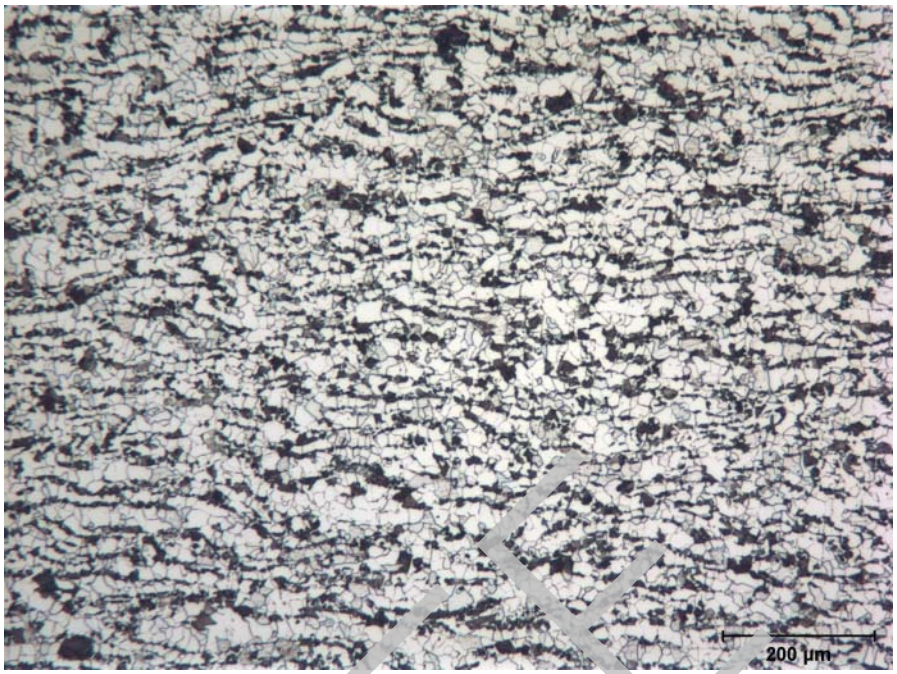

Etchant: 2% Nital Magnification: 100X

(a)

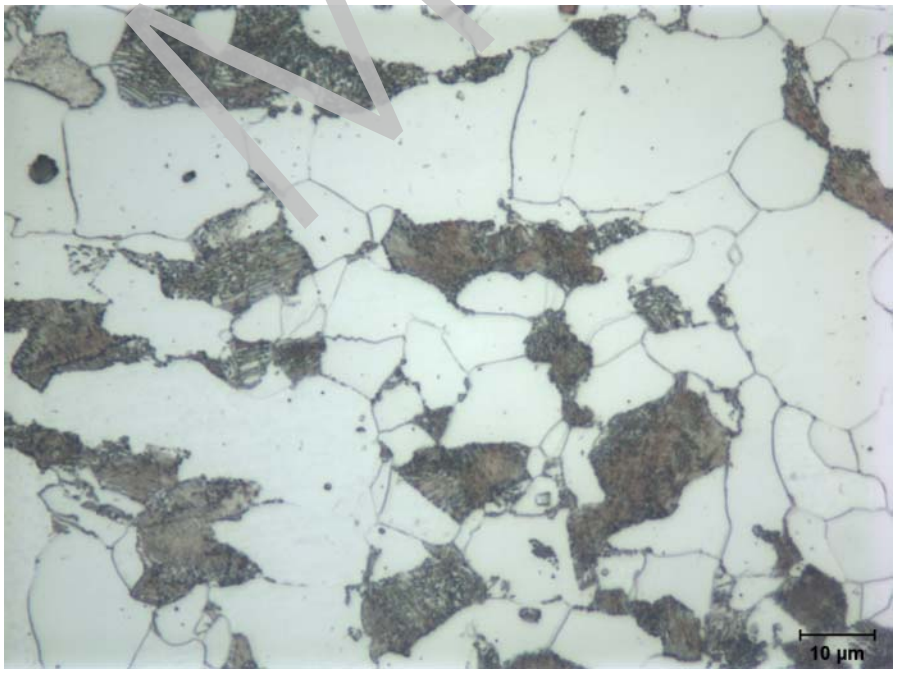

Etchant: 2% Nital Magnification: 1,000X

(b)

Figure 11 Mmicrostructure of the tube metal on the cold side of the tube.

(a) Before

(b) After

Figure 12 Ring section removed from tube near through-wall crack - as cut (a) and after flattening (b). The hot side is on the top of the ring in both images.

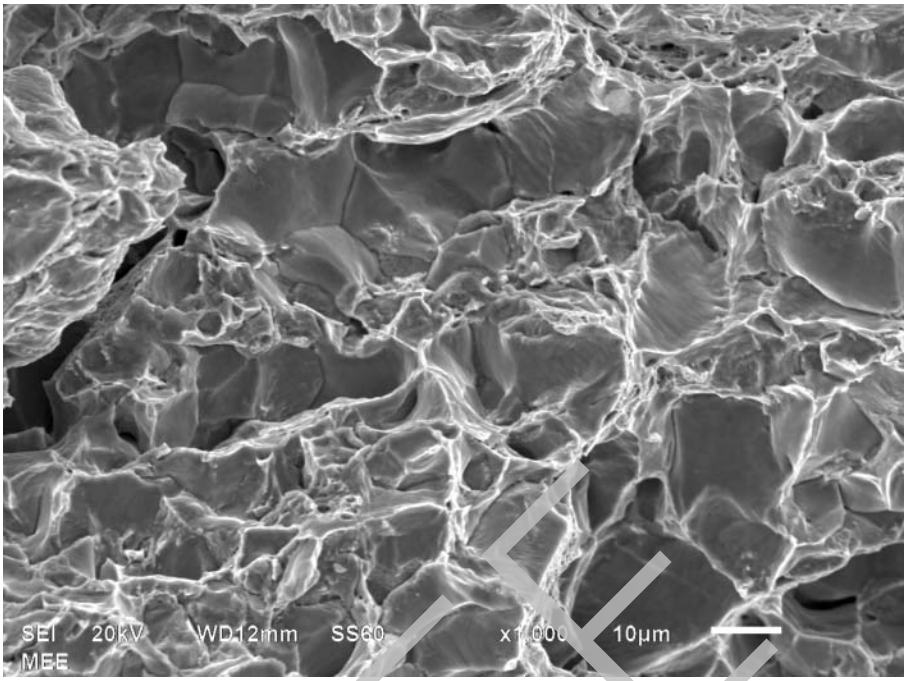

Secondary Electron Image Magnification: 1,000X

(a) Near inner surface

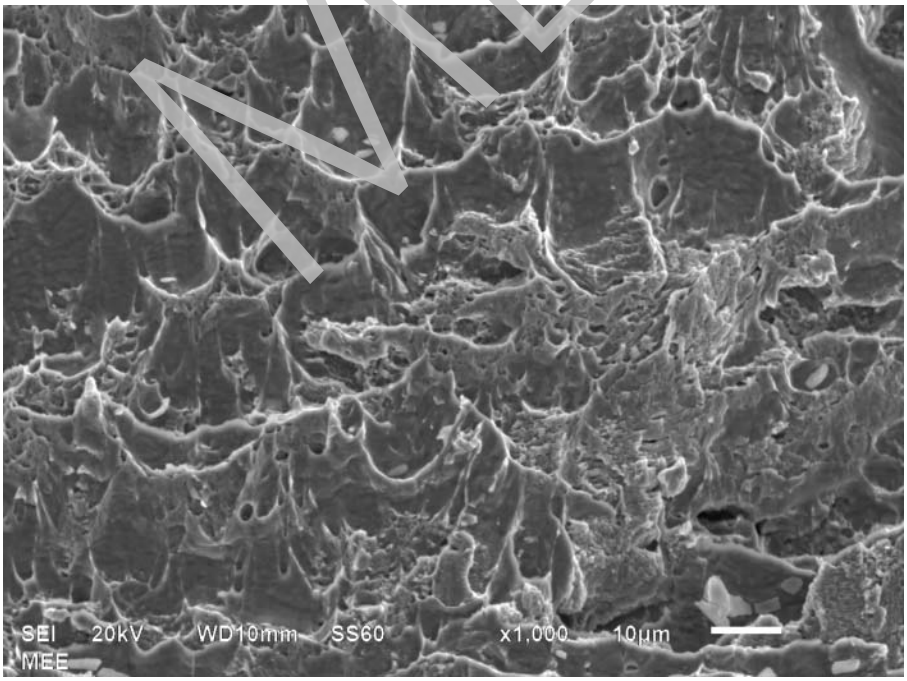

Secondary Electron Image Magnification: 1,000X

(b) Near outer surface

Figure 13 Microscopic features of the laboratory fracture at the indicated locations.

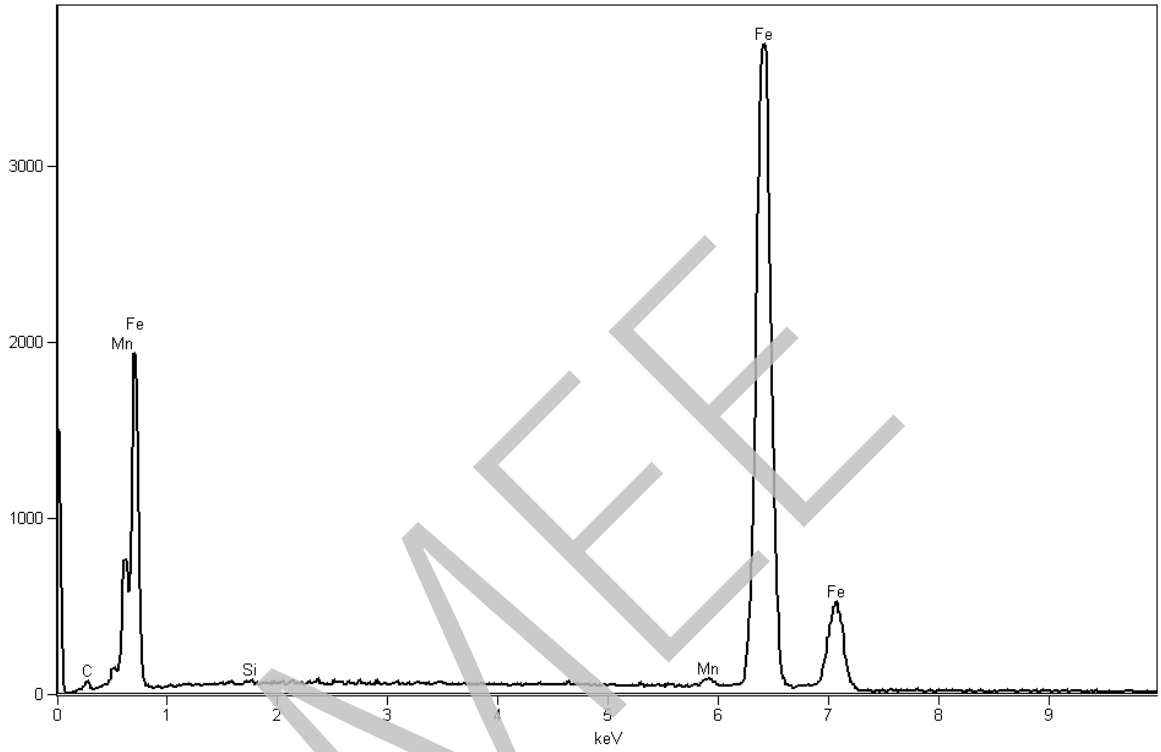

Figure 14 Spectrum for EDS analysis of the base metal at the laboratory fracture surface.

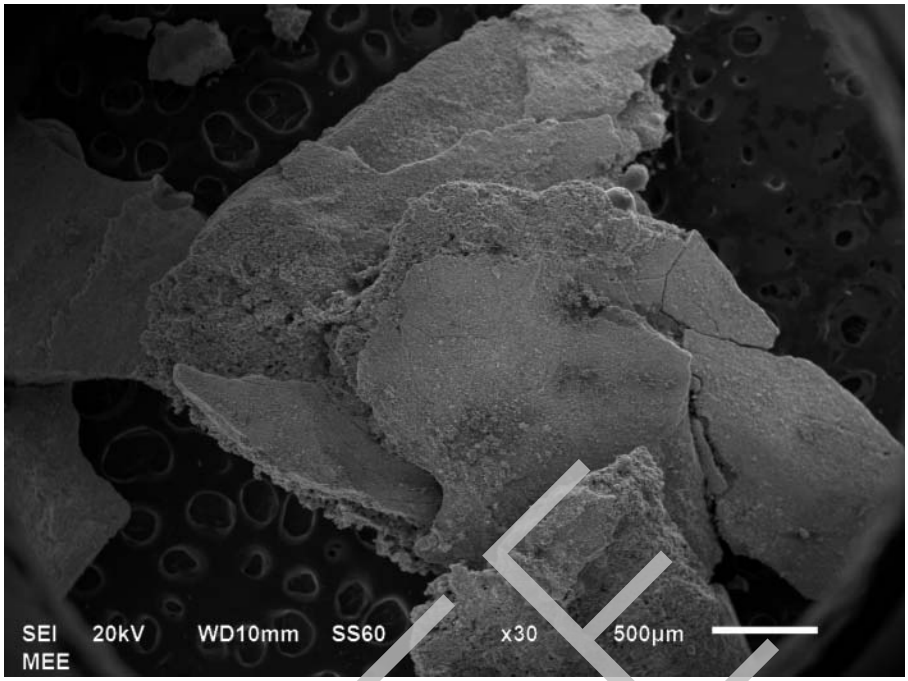

Secondary Electron Image Magnification: 30X

Figure 15 SEM image of the nonmetallic material scraped from the inner surface of the hot side of the tube.

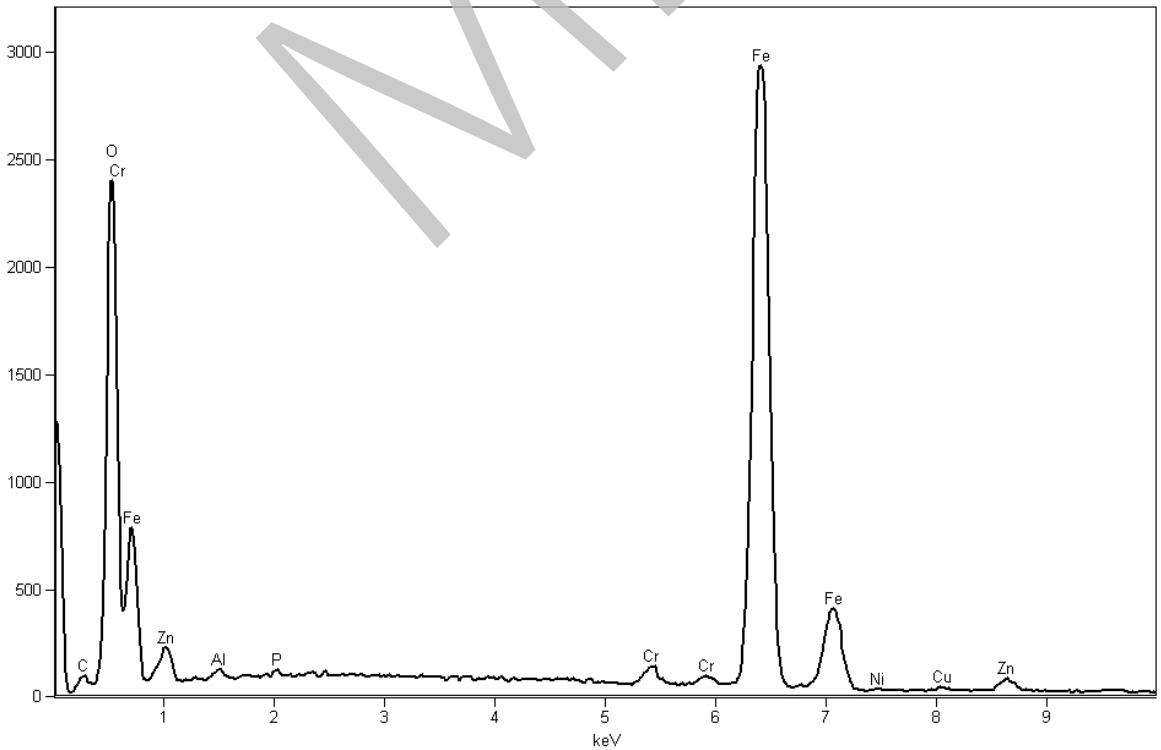

Figure 16 Spectrum for EDS analysis of the material scraped from the inner surface of the hot side of the tube.